

ENABLING RESEARCH PROJECT ENR-MAT.01.VR

# Electronic interactions of slow ions and their influence on defect formation & sputter yields for plasma facing components

**E. Pitthan<sup>1</sup>, M. V. Moro<sup>1</sup>, J. Shams-Latifi<sup>1</sup>, P. M. Wolf<sup>1</sup>, B. Bruckner<sup>1</sup>, T. Tran<sup>1</sup>, D. Moldarev<sup>1</sup>, P. Ström<sup>1</sup>, D. Primetzhofer<sup>1</sup>, P. Petersson<sup>2</sup>, M. Rubel<sup>2</sup>, C. Cupak<sup>3</sup>, M. Fellingner<sup>3</sup>, F. Aumayr<sup>3</sup>, L. Caveglia Curtil<sup>4</sup>, E. Ponomareva<sup>4</sup>, T. Malykhina<sup>4</sup>, A. Aro<sup>4</sup>, A. Sand<sup>4</sup>**

<sup>1</sup>Department of Physics and Astronomy, Uppsala University, 751 20 Uppsala, Sweden

<sup>2</sup>Department of Fusion Plasma Physics, KTH Royal Institute of Technology, 100 44 Stockholm, Sweden

<sup>3</sup>TU Wien, Institute of Applied Physics, Fusion@ÖAW, 1040 Vienna, Austria

<sup>4</sup>Department of Applied Physics, Aalto University, Aalto, Espoo FI-00076, Finland

**24 October 2024, EUROfusion Science Meeting on results of Enabling Research Projects 2021-2024**



This work has been carried out within the framework of the EUROfusion Consortium, funded by the European Union via the Euratom Research and Training Programme (Grant Agreement No 101052200 — EUROfusion). Views and opinions expressed are however those of the author(s) only and do not necessarily reflect those of the European Union or the European Commission. Neither the European Union nor the European Commission can be held responsible for them.

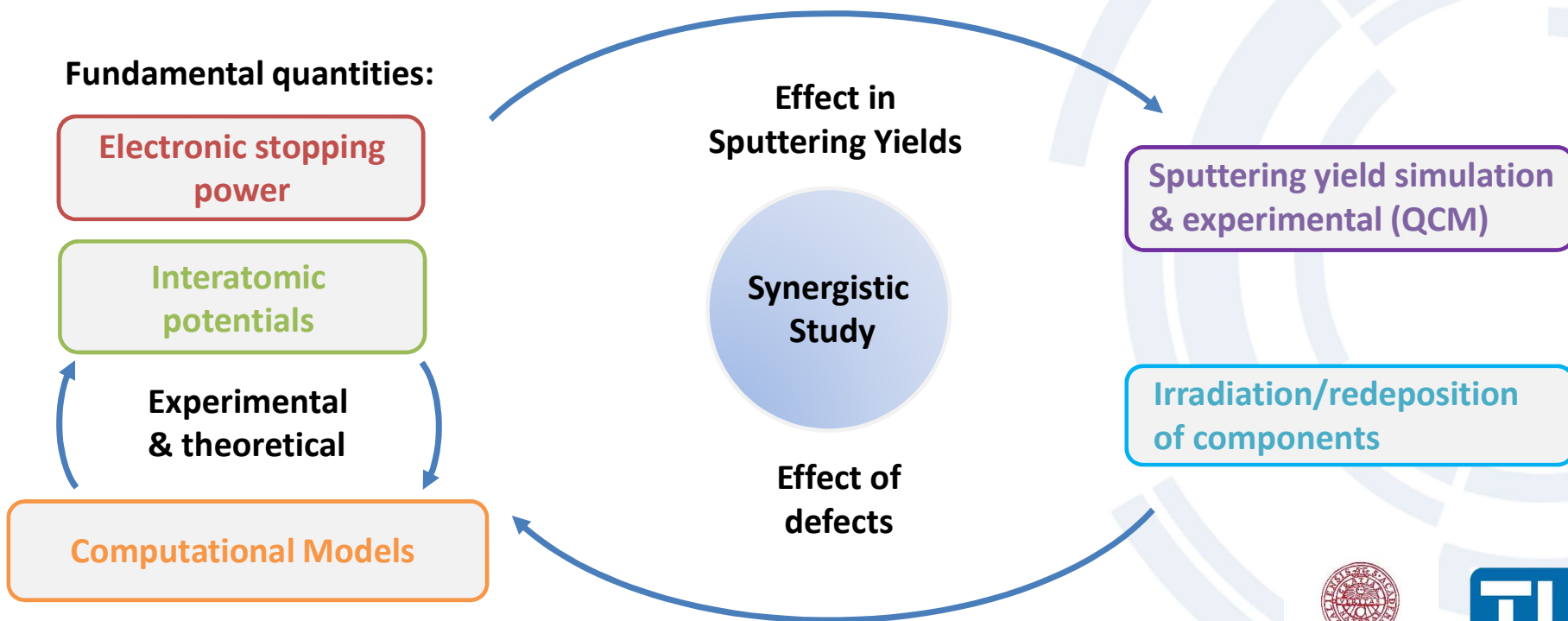




# Aim

To investigate underlying quantities fundamental for sputtering and defect formation from plasma-wall interaction:

- Important input variables in modelling of erosion and implantation in plasma facing components.
- Essential for precise material characterization using ion beam analyses.



UPPSALA  
UNIVERSITET





## Team: 2021-2024

VR	ÖAW	VTT
Eduardo Pitthan (PI)	Martina Fellingner	Andrea Sand
Jila Shams-Latifi	Johannes Brötzner	Evgeniia Ponomareva
Philipp M. Wolf	Christian Cupak	Ludovico Caveglia Curtil
Petter Ström	Richard Wilhelm	Tetiana Malykhina
Per Petersson	Friedrich Aumayr	Akseli Aro

**Start:** May of 2021.

**VR main tasks:** Sample preparation and characterization, electronic loss measurements, interatomic potential measurements, and ion irradiation experiments.

**ÖAW main tasks:** Sputtering yield measurements, and BCA-based simulations.

**VTT main tasks:** Computational modelling (simulations of electronic stopping power & MD sputtering yields).





## This presentation

### Energy losses

Background and motivation.  
Experimental procedure.  
Experimental results.  
Theoretical results (TD-DFT).

### Interatomic potentials

Background and motivation.  
Experimental/modelling procedure.  
Experimental results.  
Comparison with current models.

### Sputtering yields

Experimental procedure.  
Experimental results.  
Comparison with BCA simulations.  
Effect of fundamental quantities in  
BCA simulations.



## Aim: Energy losses

Important fundamental quantity for simulation of PWI:

$-dE/dx$  → Stopping Power (energy loss per unity path).

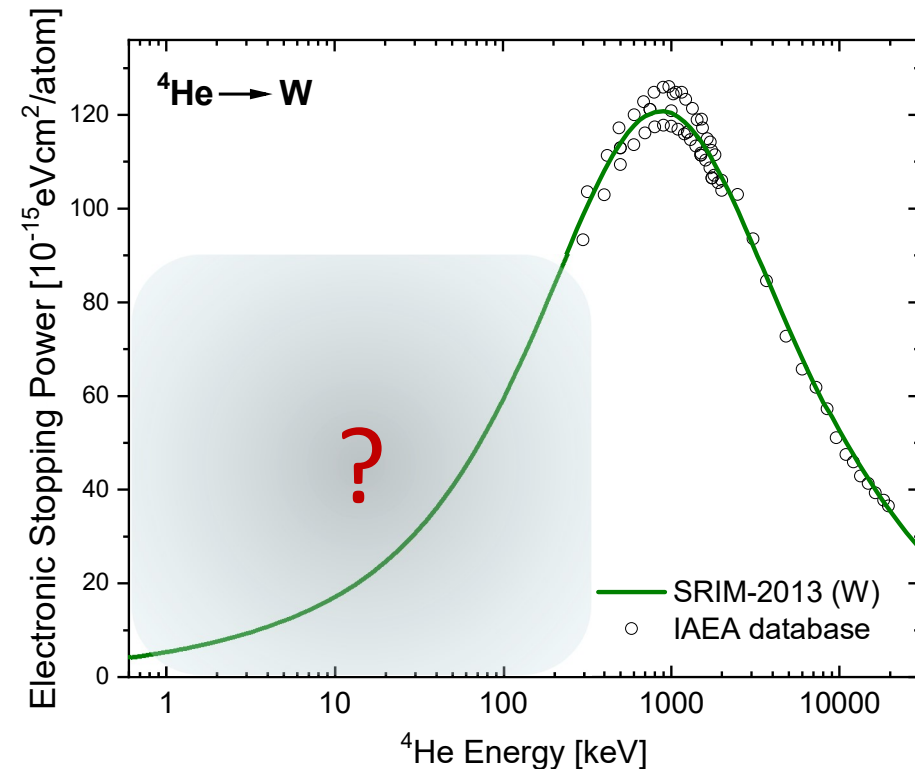
$\varepsilon = -\frac{1}{N} \frac{dE}{dx}$  → Stopping cross section (independent of density).

Semi-empirical models (such as used in SRIM code [1]) use available experimental data...

First wall in DEMO:



- Only one dataset below 300 keV (M. Moro-UU, 2022).
- Limited experimental information at low energy ranges.
- For Fe-Cr alloys: No experimental data at any energy.



Electronic Stopping Power of Matter for Ions:  
available data from International Atomic Energy Agency (IAEA) [2]  
(Mor21 database removed – this work)

[1] J. F. Ziegler et al. Nucl. Instr. Meth. Phys. Res. B, 268, 1818-1823 (2010).

[2] [https://www-nds.iaea.org/stopping/stopping\\_hydr.html](https://www-nds.iaea.org/stopping/stopping_hydr.html).

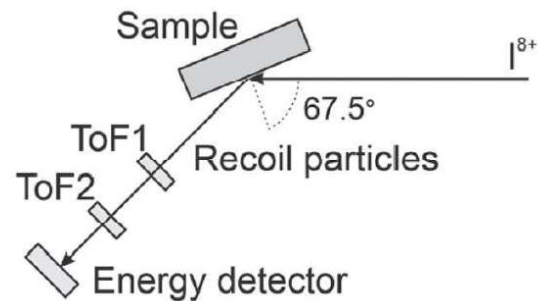




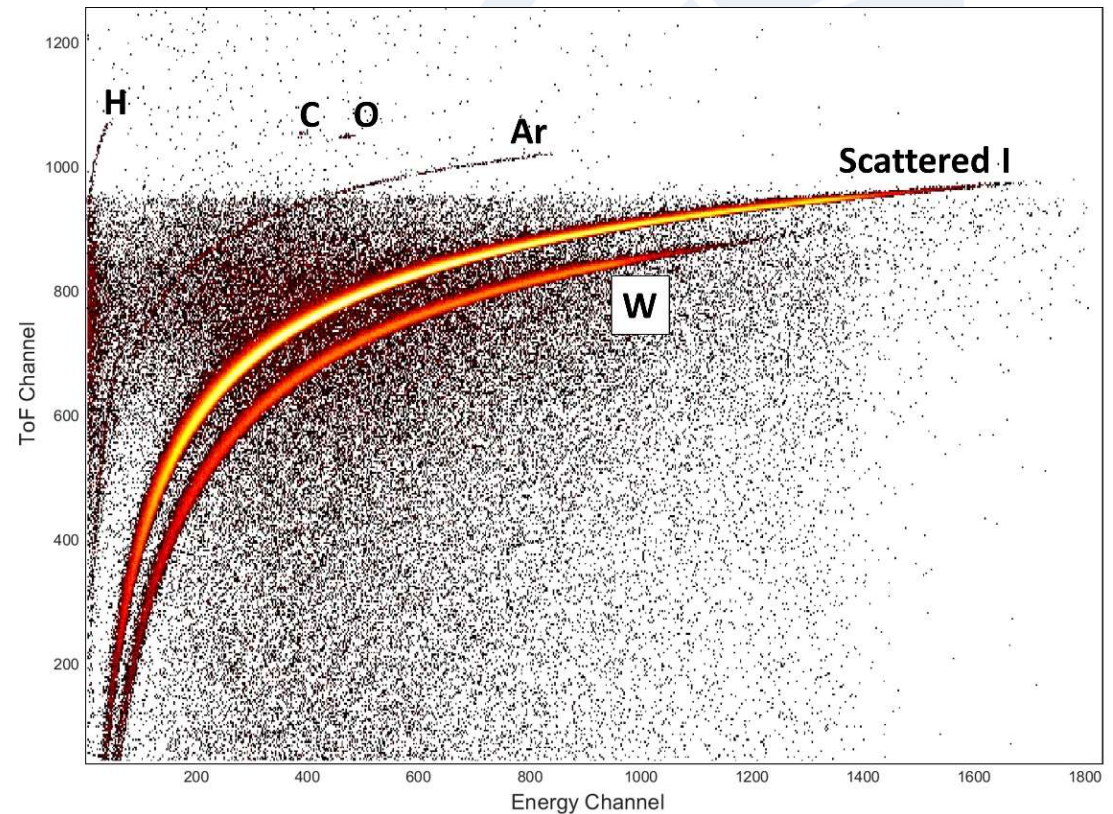
## Sample preparation/characterization

*Characterization of the chemical composition of the pristine samples (Fe, W, EUROFER) by combined ion beam based techniques (UU), as a protocol for the standard quality control.*

→ Atomic concentration depth profiles by ToF-ERDA:



**Example:** ToF-ERDA spectrum from sputter-deposited W film.

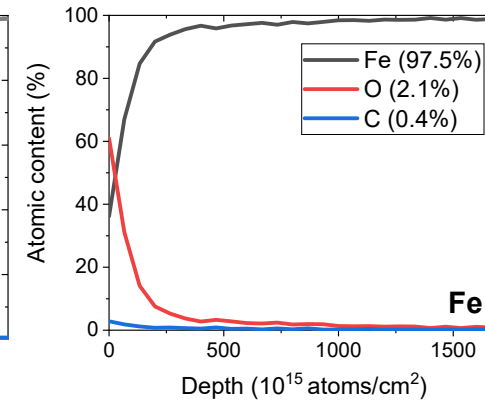
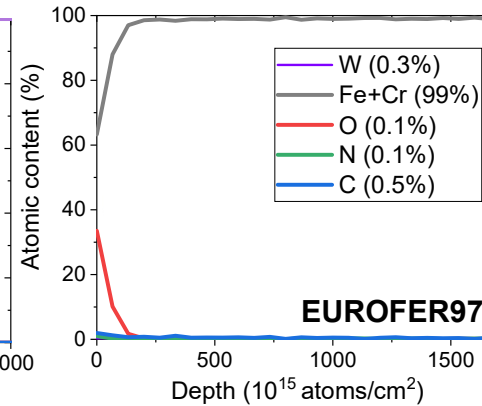
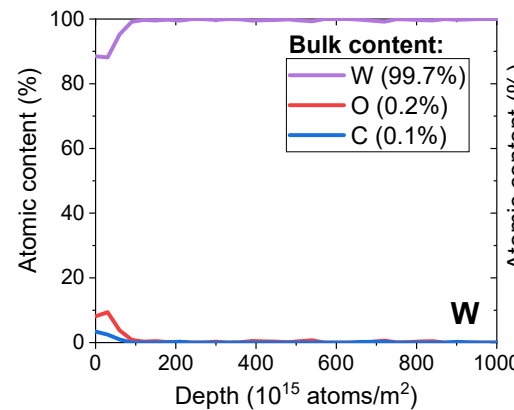
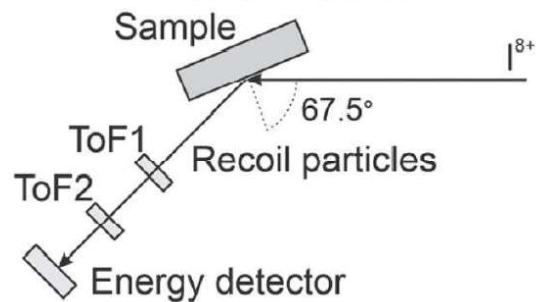




# Sample preparation/characterization

Characterization of the chemical composition of the pristine samples (Fe, W, EUROFER) by combined ion beam based techniques (UU), as a protocol for the standard quality control.

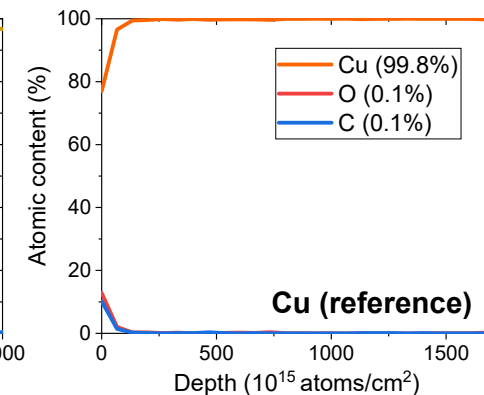
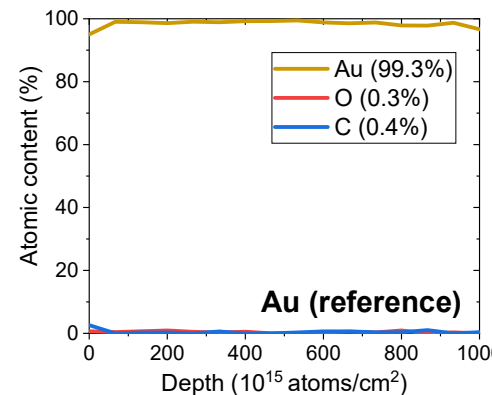
## → Atomic concentration depth profiles by ToF-ERDA:



→ Low impurity concentrations in bulk.  
 Evaluation window  $500-1000 \times 10^{15} \text{ atoms/cm}^2$

Final stopping data corrected by Bragg's rule:

$$\epsilon^{A_m B_n \dots} = m\epsilon^A + n\epsilon^B + \dots$$





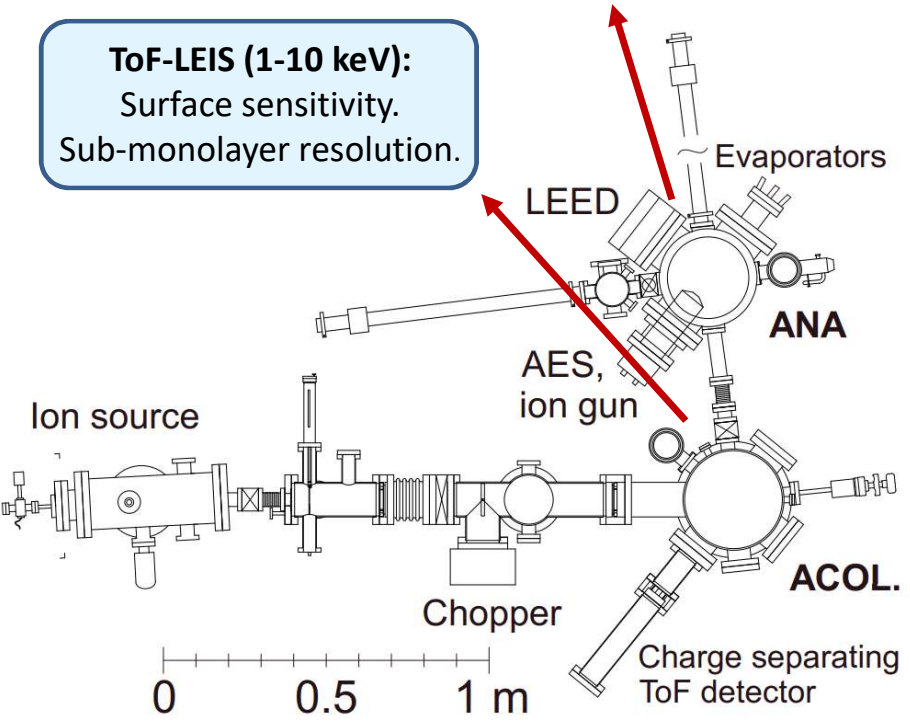
# Electronic energy loss measurements

Experimental procedure for low energy regime

## ACOLISSA experimental set-up:

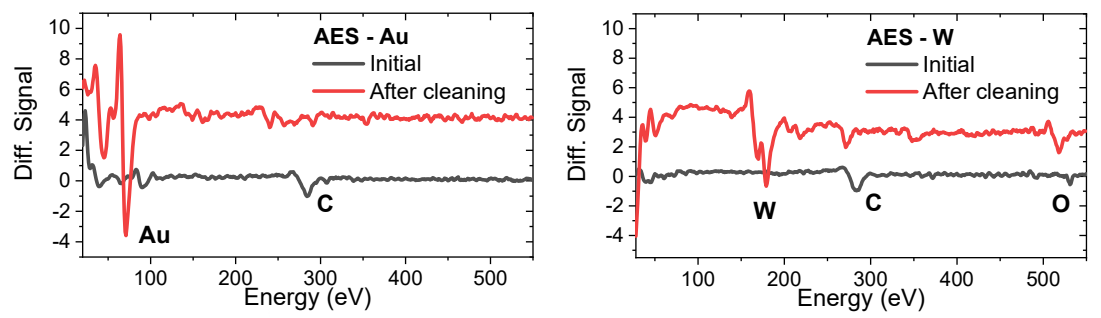
**Analytical Chamber:** Sputtering cleaning, annealing, AES, e-beam evaporation, and LEED.

**ToF-LEIS (1-10 keV):**  
Surface sensitivity.  
Sub-monolayer resolution.

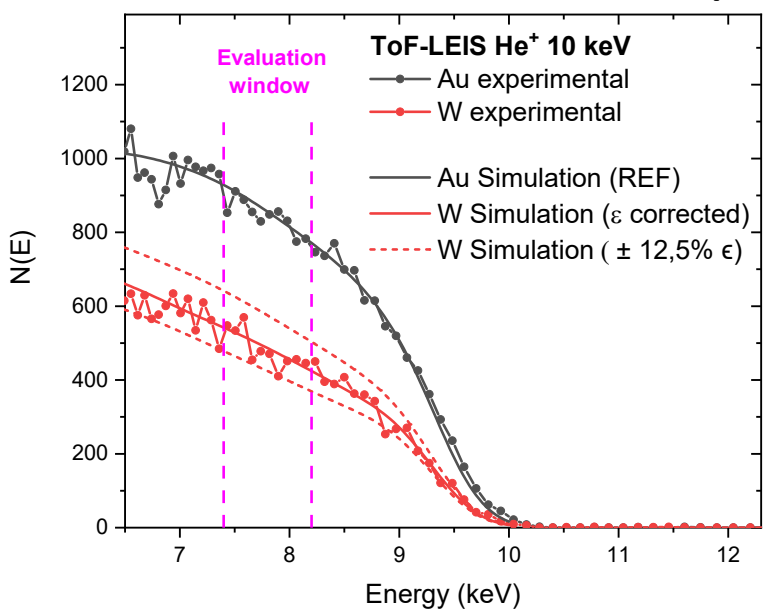


P. Ström and D. Primetzhofer 2022 JINST 17 P04011

## Sample cleaning: cycles of Ar<sup>+</sup> sputtering 3 keV 30°.



## SCS relative measurements in comparison with MC simulations:



→ Cu/Au as reference under same experimental condition.

→ SCS extraction from height ratio.

→ Similar approach for MEIS and MeV energies our laboratory.





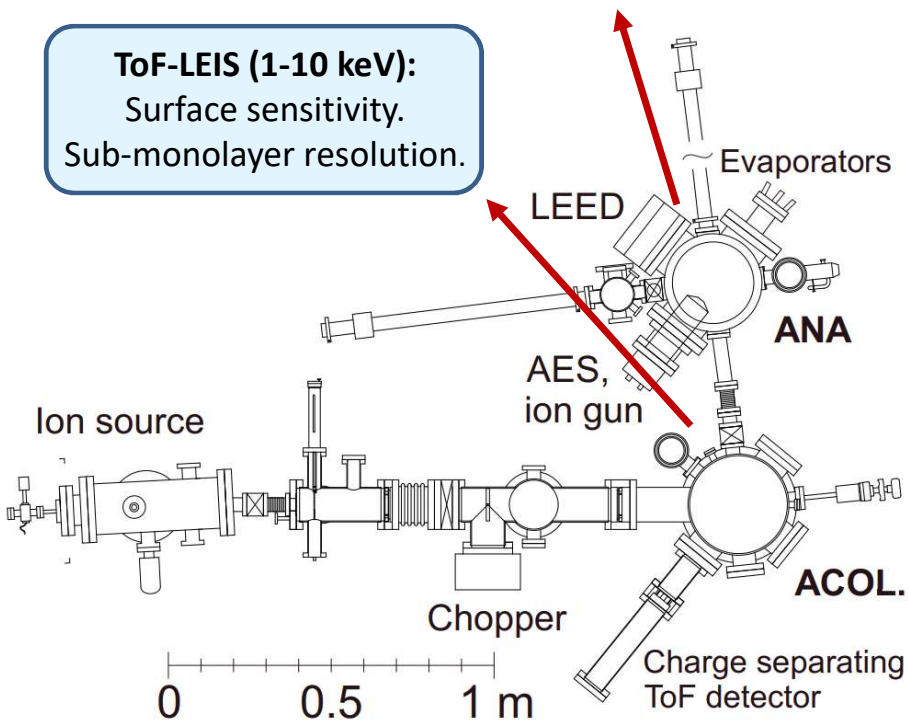
# Electronic energy loss measurements

Experimental procedure for low energy regime

## ACOLISSA experimental set-up:

**Analytical Chamber:** Sputtering cleaning, annealing, AES, e-beam evaporation, and LEED.

**ToF-LEIS (1-10 keV):**  
Surface sensitivity.  
Sub-monolayer resolution.



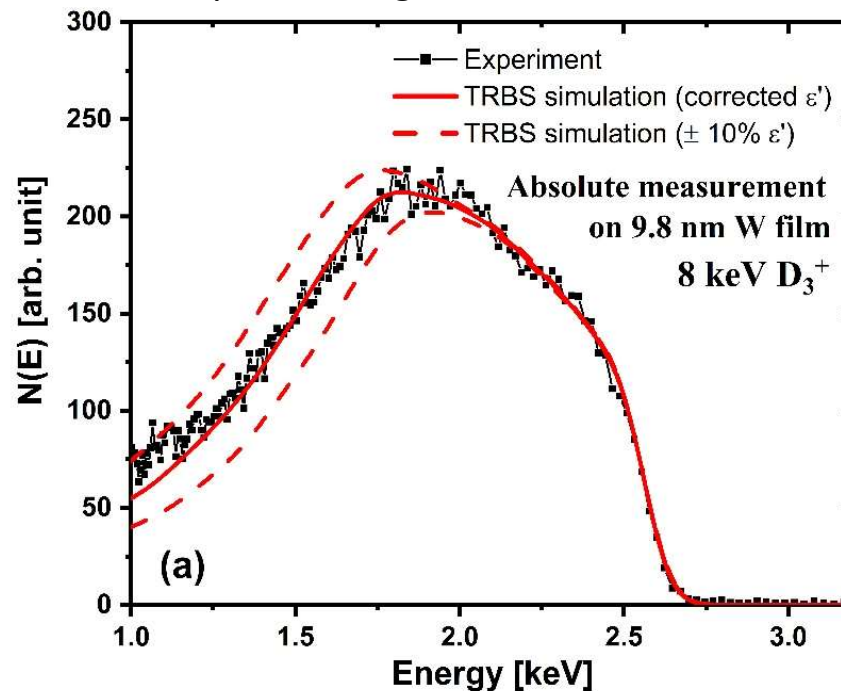
P. Ström and D. Primetzhofer 2022 JINST 17 P04011

## Complementary approach (absolute approach):

Sputter-deposited thin films of PFC on light (C and Si) substrates.

Film thickness was measured by RBS and simulated using SIMNRA to be employed in TRBS simulations.

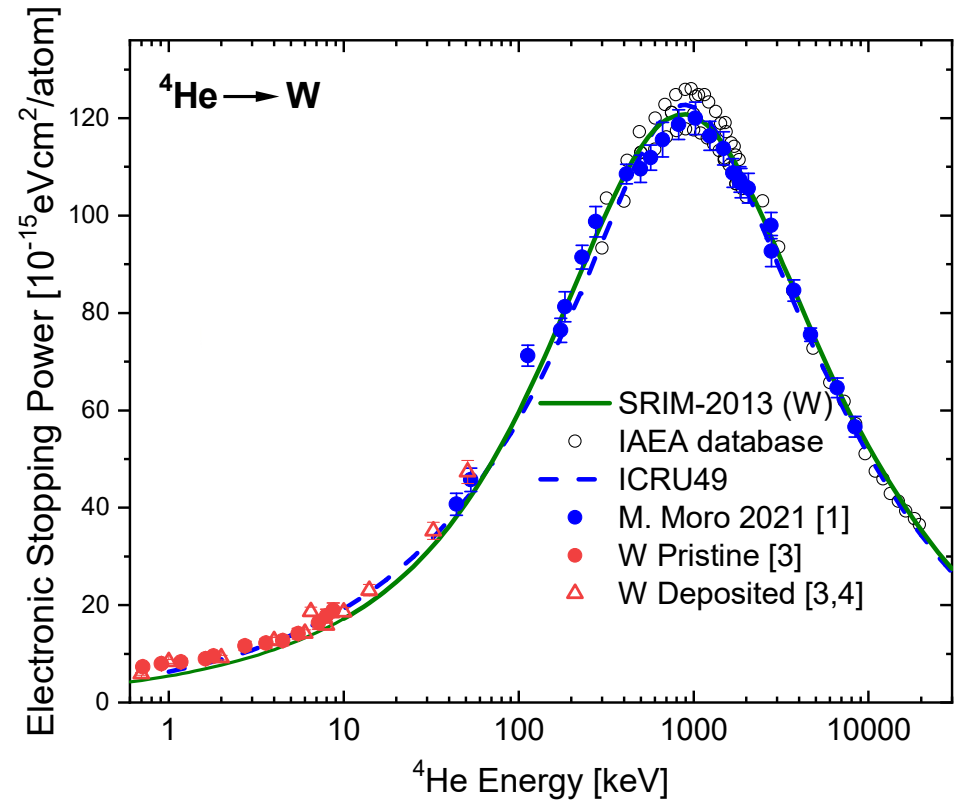
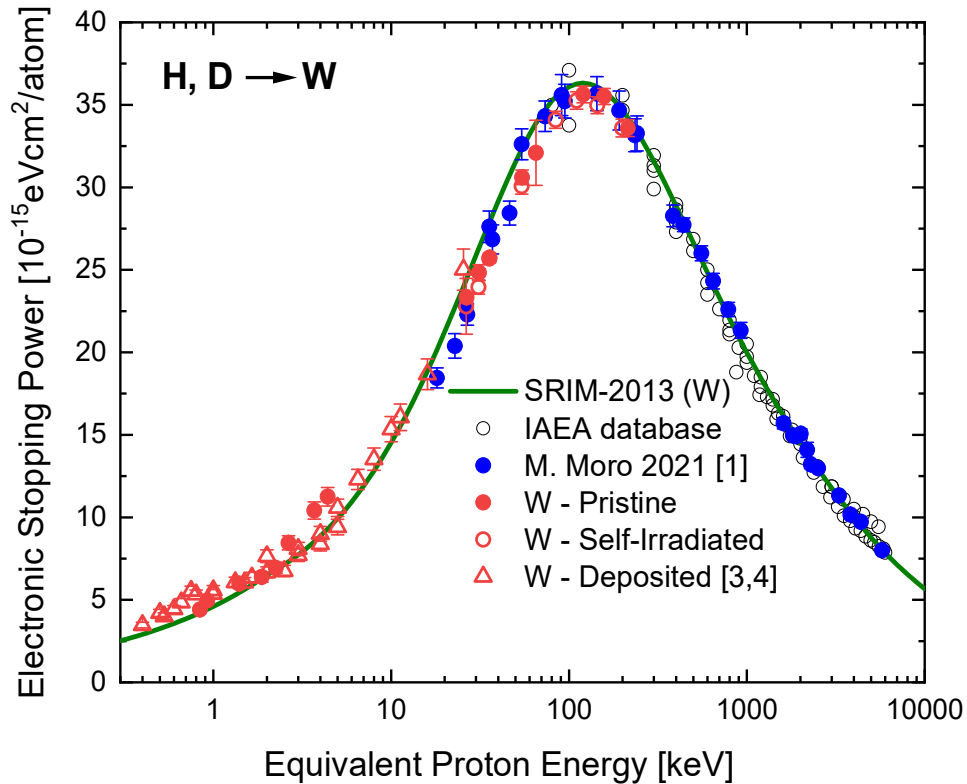
SCS from width from spectrum signal.





# Electronic energy loss measurements

Experimental stopping cross-section of pristine Fe, W, and EUROFER97



- [1] M. V. Moro et al., Nucl. Instrum. Meth B **498** (2021).  
[2] M. J. Berger, et al., Report 49, Oxford Academic (1993).  
[3] J. Shams-Latifi, et al., Nucl. Mater. and Energy **36** (2023).  
[4] E. Ponomareva, et al., Phys. Rev. B **109** (2024).

### Damage of PFC by Self-irradiation:

$W^{2+}$  2.84 MeV → W ( $1.6 \times 10^{15}$  W/cm<sup>2</sup>);

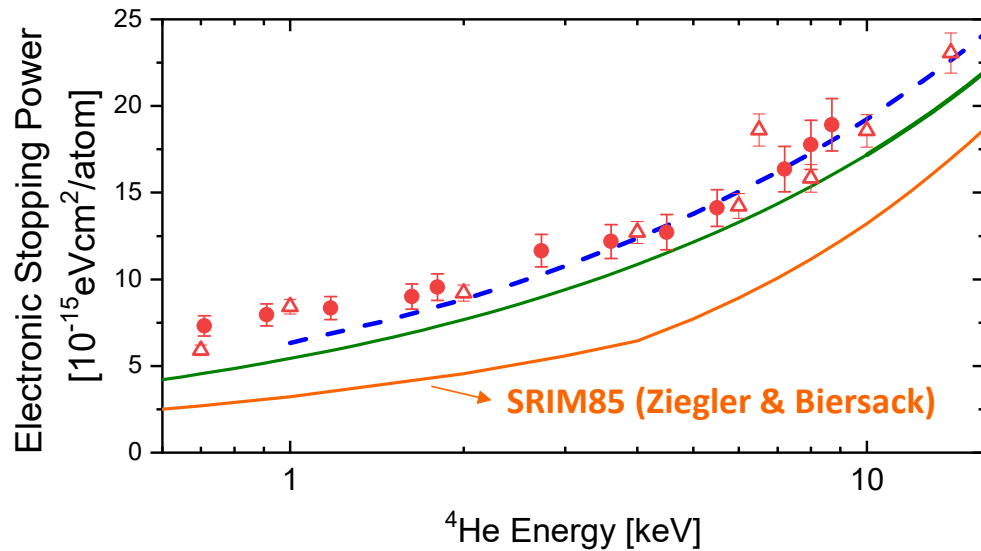
$Fe^+$  300 keV → Fe/EUROFER97 ( $42.2 \times 10^{15}$  Fe/cm<sup>2</sup>).

**No significant effect of self-irradiation observed in this work.**



# Electronic energy loss measurements

Experimental stopping cross-section of pristine Fe, W, and EUROFER97

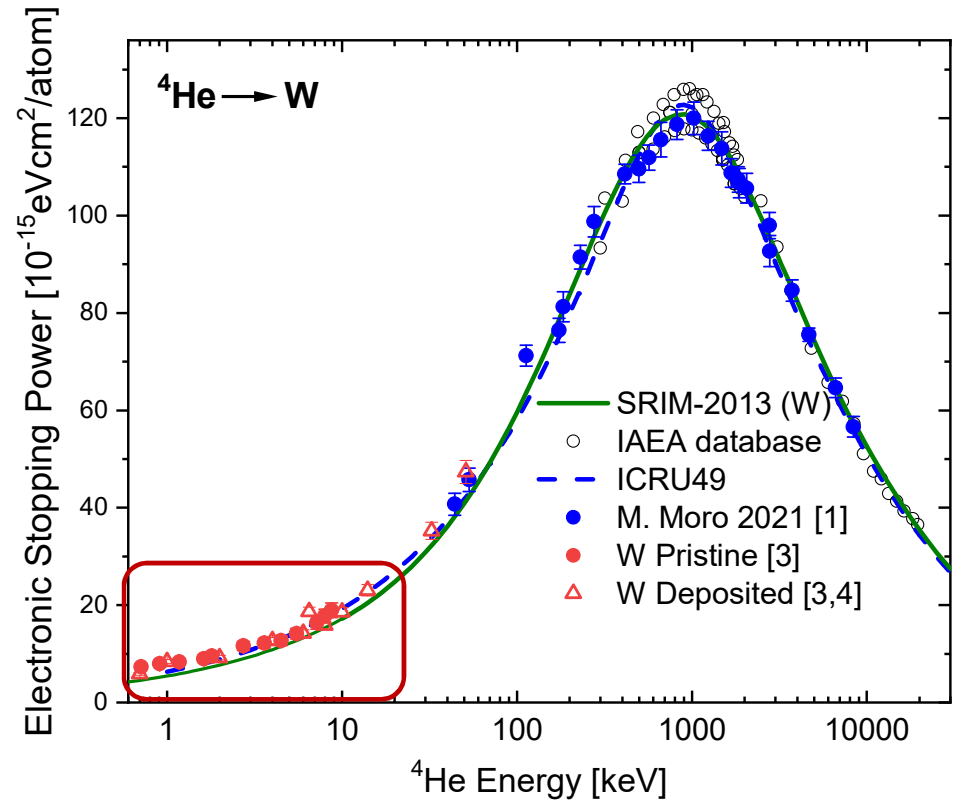


SCS at LEIS published [3,4]:

LEIS (<15 keV): Discrepancies from SRIM-2013 up to 20% for protons and 60% for He.

Discrepancies up to 210% from SRIM-1985.

- [1] M. V. Moro et al., Nucl. Instrum. Meth B **498** (2021).
- [2] M. J. Berger, et al., Report 49, Oxford Academic (1993).
- [3] J. Shams-Latifi, et al., Nucl. Mater. and Energy **36** (2023).
- [4] E. Ponomareva, et al., Phys. Rev. B **109** (2024).



Damage of PFC by Self-irradiation:

$\text{W}^{2+}$  2.84 MeV  $\rightarrow$  W ( $1.6 \times 10^{15}$  W/cm<sup>2</sup>);

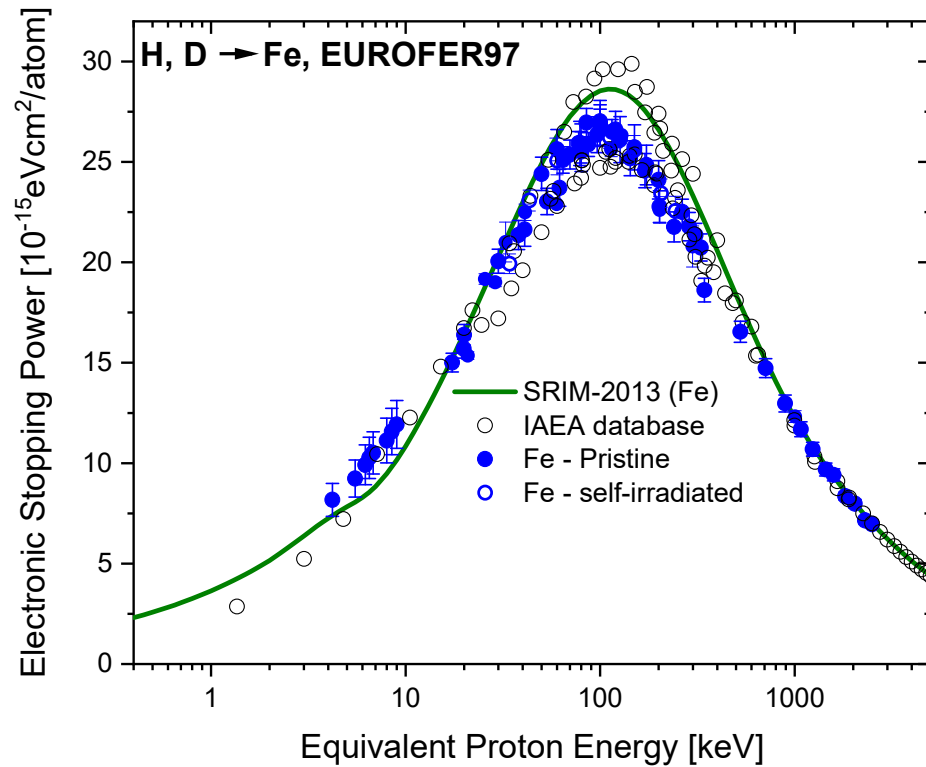
$\text{Fe}^+$  300 keV  $\rightarrow$  Fe/EUROFER97 ( $42.2 \times 10^{15}$  Fe/cm<sup>2</sup>).

No significant effect of self-irradiation observed in this work.



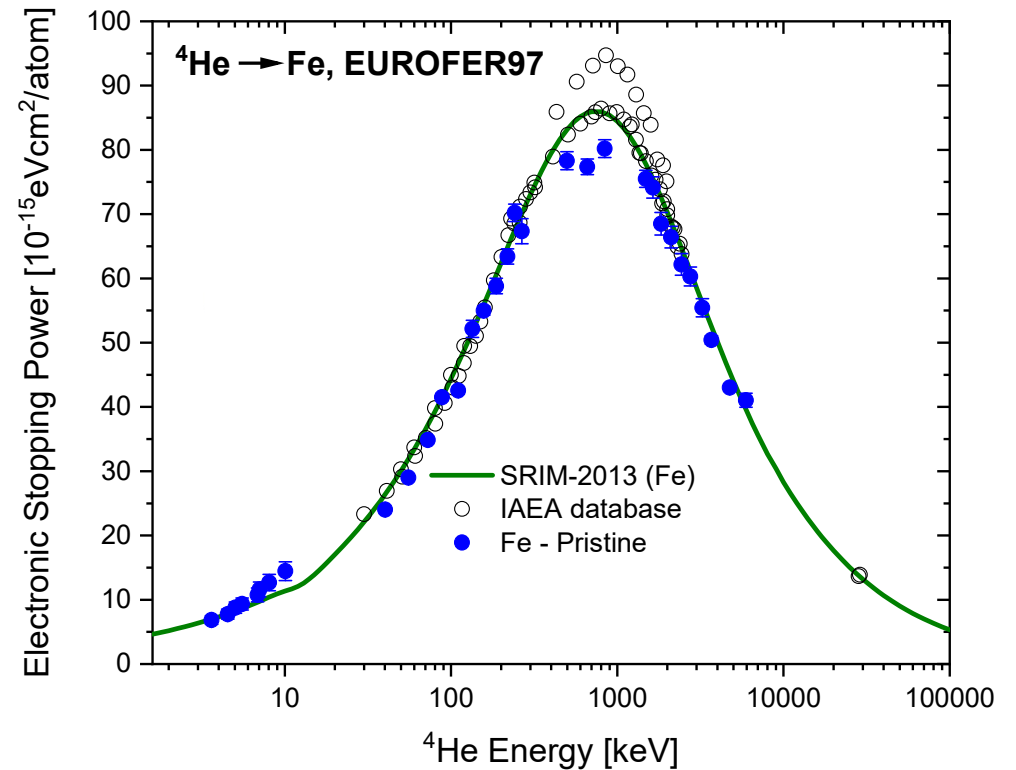
# Electronic energy loss measurements

Experimental stopping cross-section of pristine Fe, W, and EUROFER97



$H^+ \rightarrow Fe$

- Good agreement at MeV range.
- Large discrepancy with SRIM around maximum (up to 11%).
- Large discrepancy with SRIM at low energy range (up to 20%).



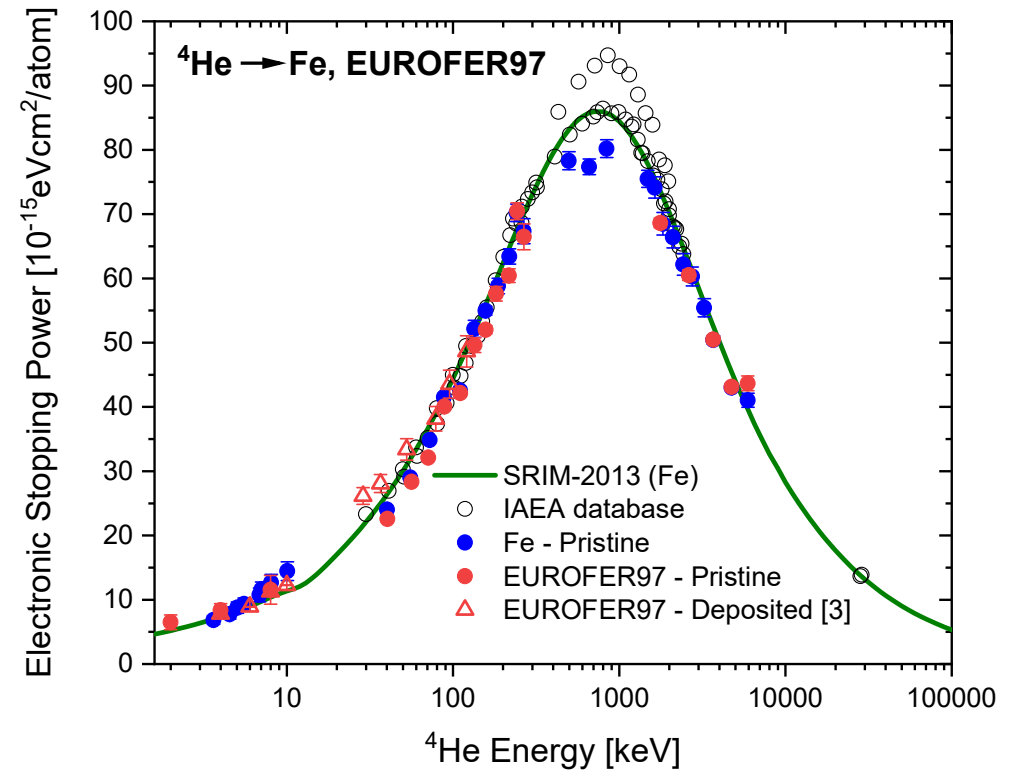
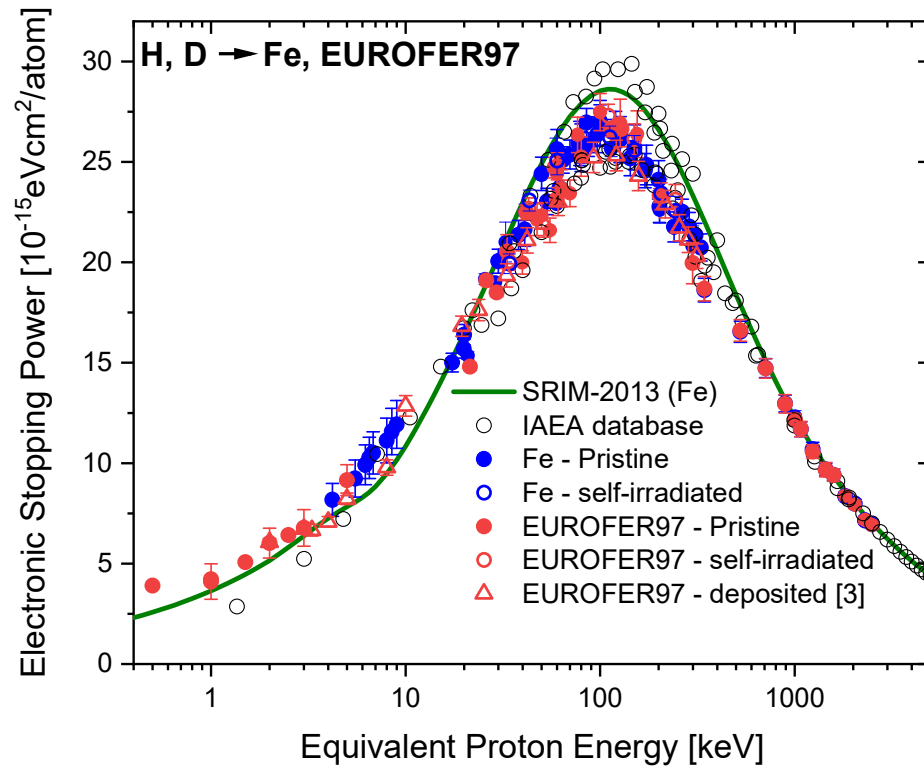
$He^+ \rightarrow Fe$

- Good agreement at keV/MeV range within 6%.
- LEIS: discrepancy up to 26%.



# Electronic energy loss measurements

Experimental stopping cross-section of pristine Fe, W, and EUROFER97



## H<sup>+</sup> → Fe, EUROFER97

Similar behaviour between Fe and EUROFER97  
No significant discrepancy from Bragg's rule.



# Electronic energy loss: TD-DFT simulations

Theoretical stopping power of pristine W, Fe, and Fe-Cr

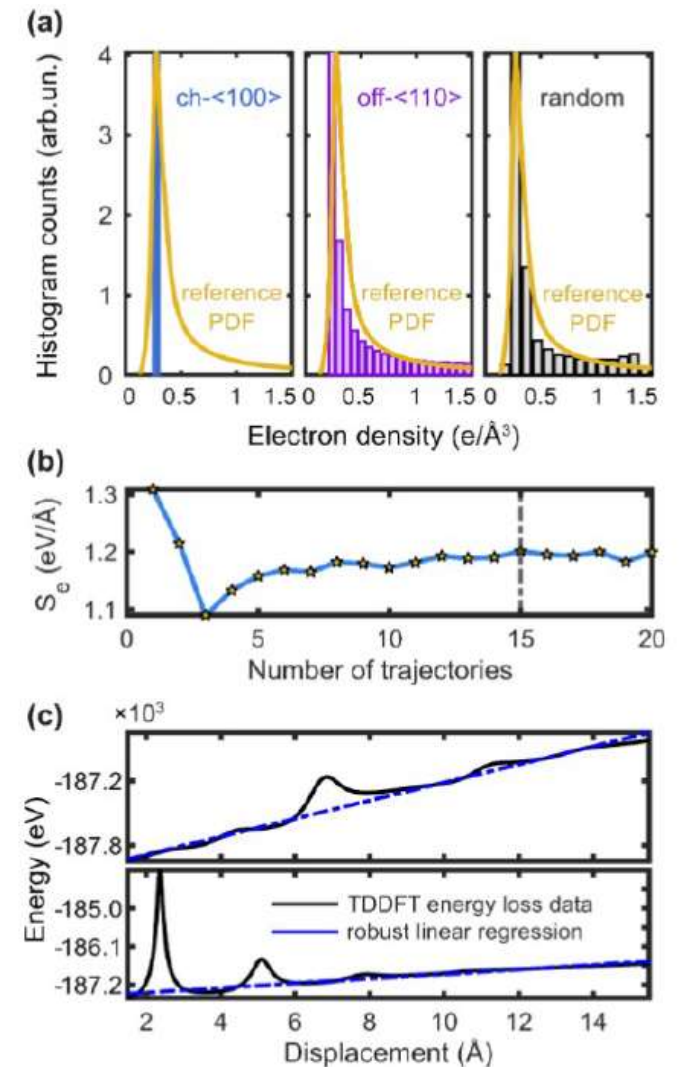
Theoretical calculation of electronic stopping power for random trajectories of light ions in pristine W, Fe and Fe-alloys using TD-DFT calculations.

Electronic stopping power from rate of change of total energy of the system, with ion travelling at constant velocity.

Simulation cell: 6x3x3 supercell (i.e. 108 W + 1 H atoms).  
Qb@ll TDDFT code + LDA norm-conserving pseudopotentials.  
lattice constant  $a$  with impact parameter  $b$ .

Method for selecting **random trajectories** sampling of different impact parameters aiming to capture all possible energy loss pathways between the ion and target atoms.

E. Ponomareva et al., Phys. Rev. B **109** (2024).







# Electronic energy loss: TD-DFT simulations

Theoretical stopping power of pristine W, Fe, and Fe-Cr

Systematic investigation of the influence of **ion-target geometry** (channelling, off-centre, and random geometries) and **core-states description** (W12 and W 20) of the target in the electronic energy losses.

Hyperchannelling trajectories are significantly lower than the experimental data.

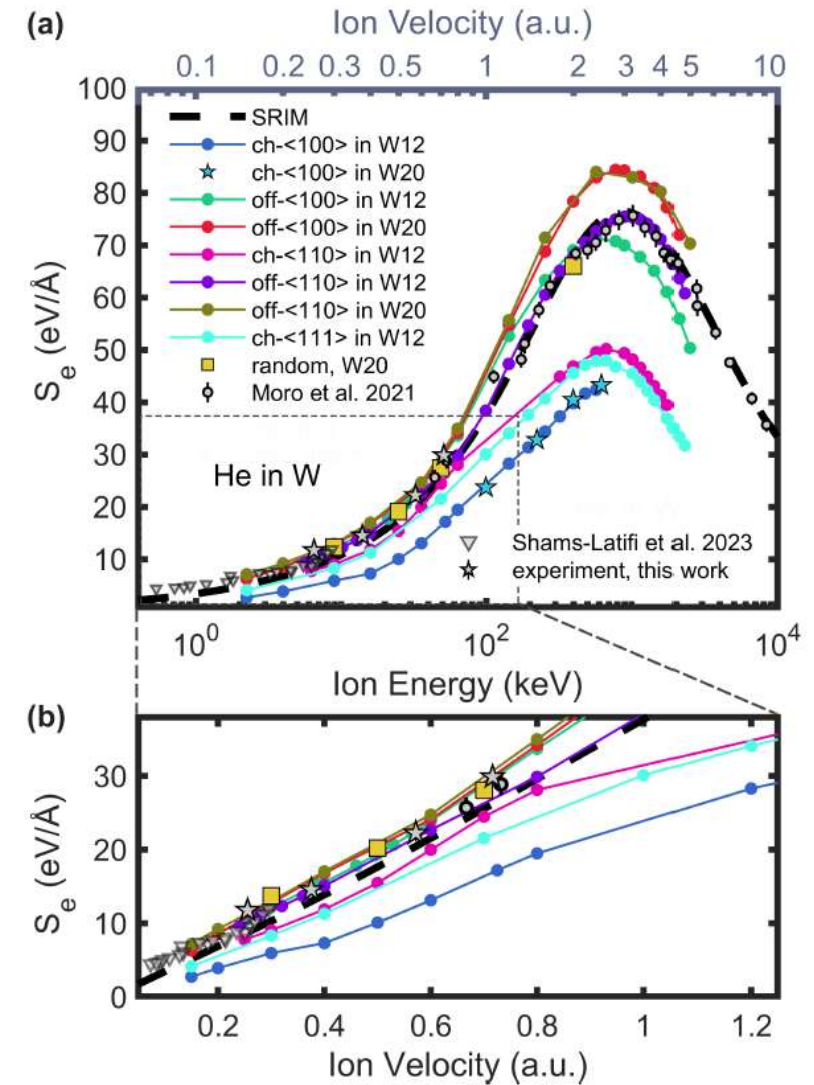
Good agreement with experimental data at lower energies.

Deviation from velocity proportionality for both projectiles traversing the hyperchannelling directions can be explained through the existence of a threshold velocity leading to the activation of semicore states.

## Additional observations:

Vacancies and Cr in Fe-Cr found to have negligible effect on stopping power → in agreement with experimental observations.

E. Ponomareva et al., Phys. Rev. B **109** (2024).





# Interatomic potentials

## Motivation and Theoretical Background

At low energies, interactions with electrons cannot be neglected.

### The screened Coulomb potential:

$$V(r) = \underbrace{\frac{Z_p Z_t e^2}{r}}_{\text{Coulomb potential}} \times \underbrace{\phi\left(\frac{r}{a}\right)}_{\text{Screening function}}$$

### Correcting the screening length:

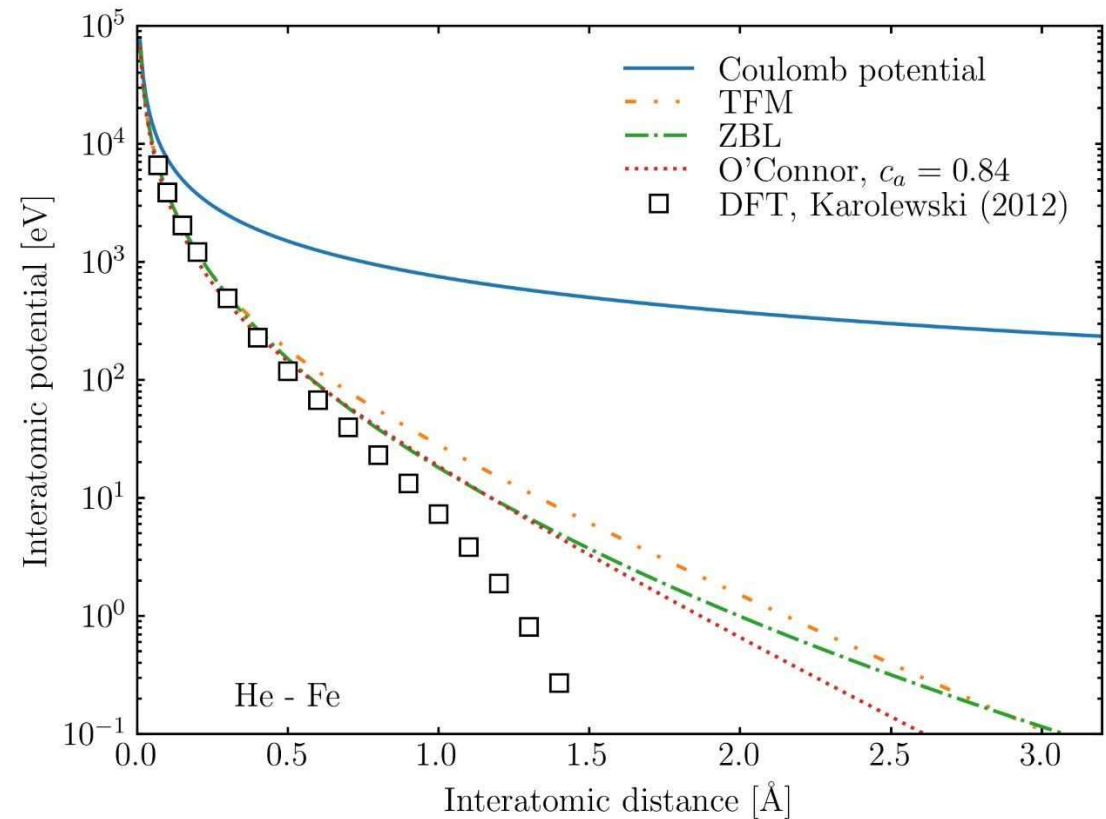
$$a = a_f \times C_a$$

$a_f$  = Firsov screening length

$C_a$  = Empirical correction factor

**Common models (TFM and ZBL) are known to present inaccuracy.**

**Lack of experimental reference data for many ion-solid combinations, to assess the quality of models for the interatomic potentials difficult.**

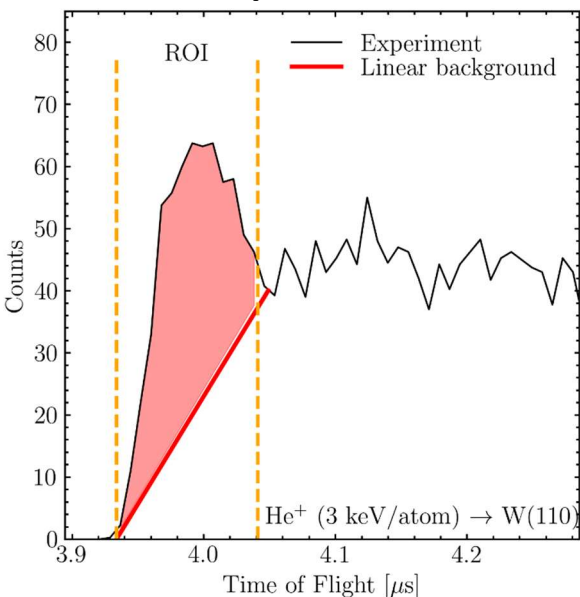




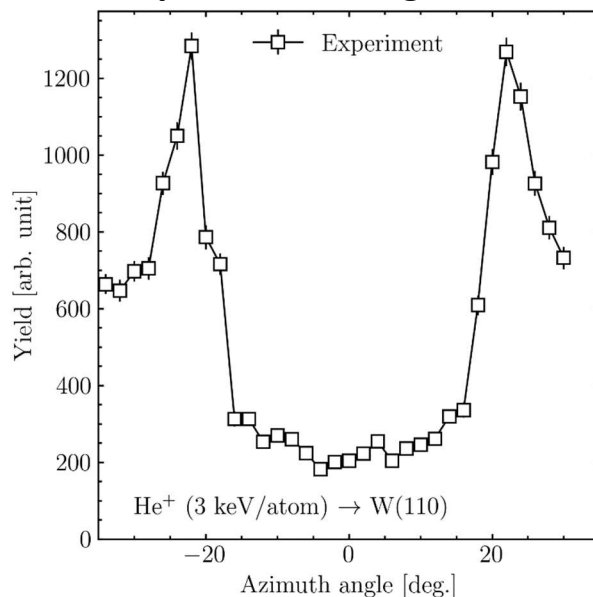
# Interatomic potentials

Experimental approach

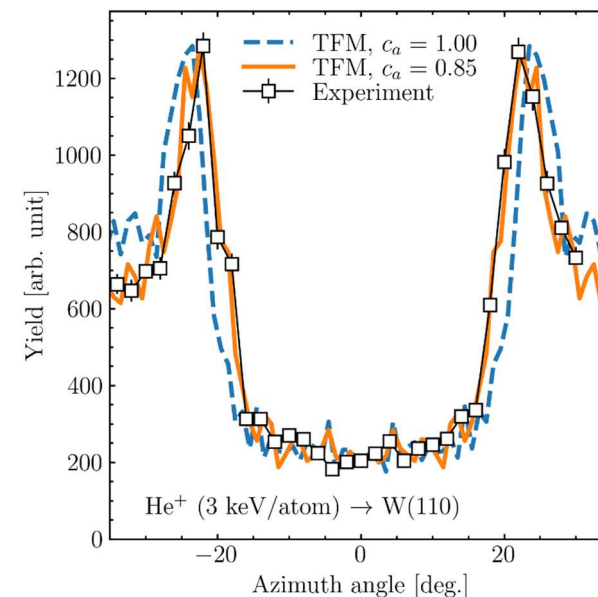
### ToF-LEIS spectrum



### Experimental angular scan

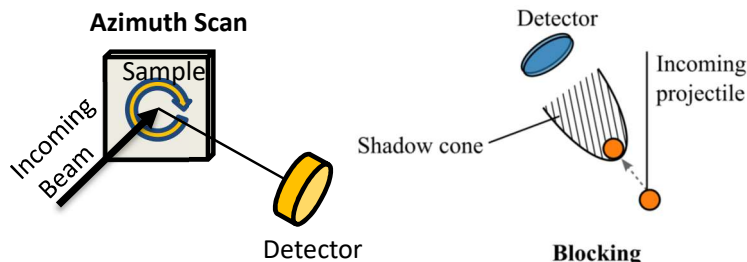


### Fit with MD simulation



After sequential steps of surface cleaning (Ar sputtering and annealing) monitored with AES/LEED.

Background subtraction: multiple scattering from deeper layers.



- | Ions:       | Single crystal surfaces: |
|-------------|--------------------------|
| • Helium    | • W(110)                 |
| • Deuterium | • Fe(100)                |

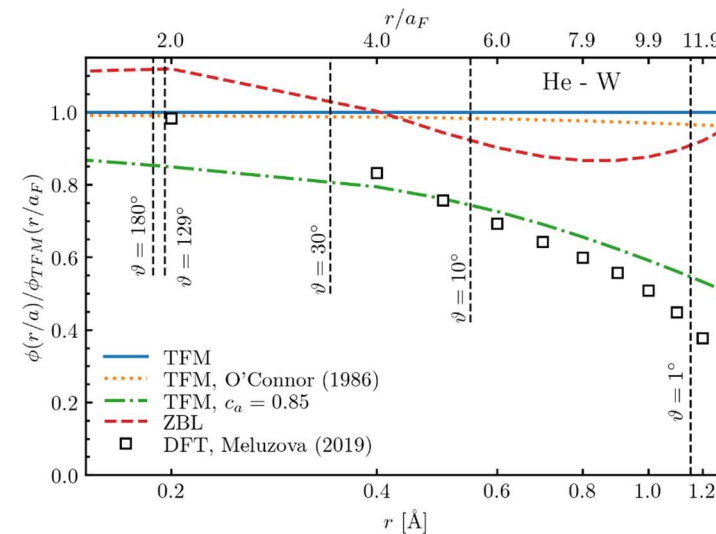
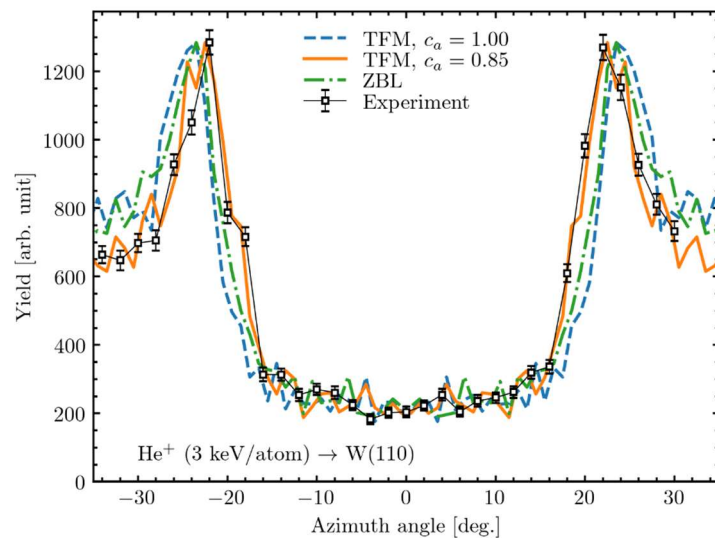
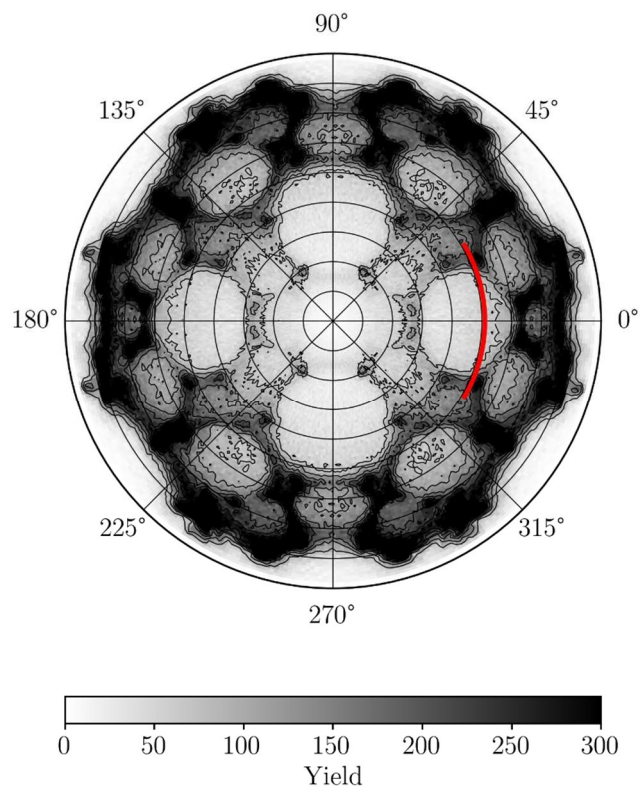
P. M. Wolf, E. Pitthan, D. Primetzhofer, submitted for publication (Pinboard 38569)



# Interatomic potentials

Results

## Helium - Tungsten



- Scan crossing [010] crystal axis of the (110) surface
- Best agreement for TFM with  $c_a=0.85$
- TFM, ZBL, and O'Connor predict higher values
- Good agreement with DFT for relevant angles

Backscattering map  
3 keV He from W(110)

P. M. Wolf, E. Pitthan, D. Primetzhofer, submitted for publication (Pinboard 38569)

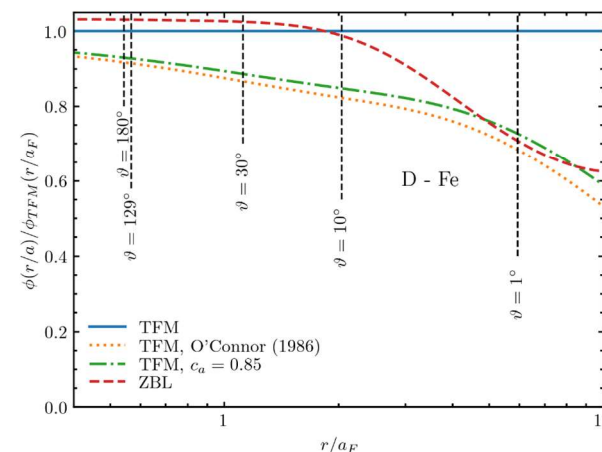
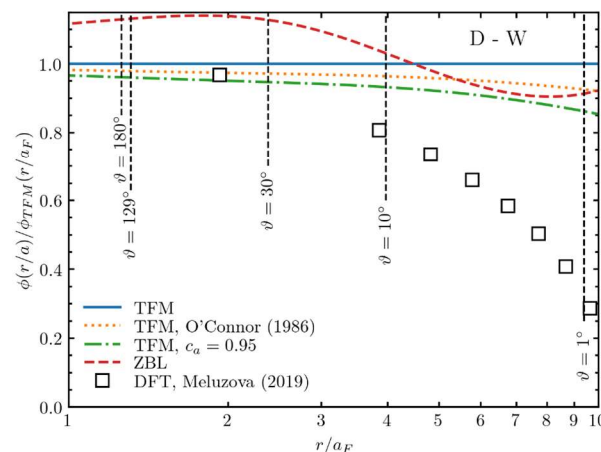
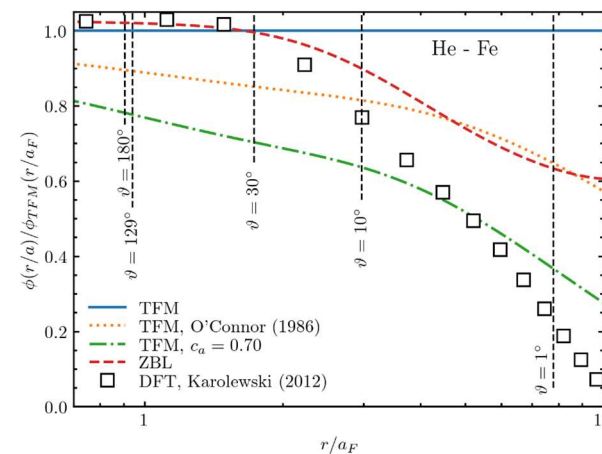
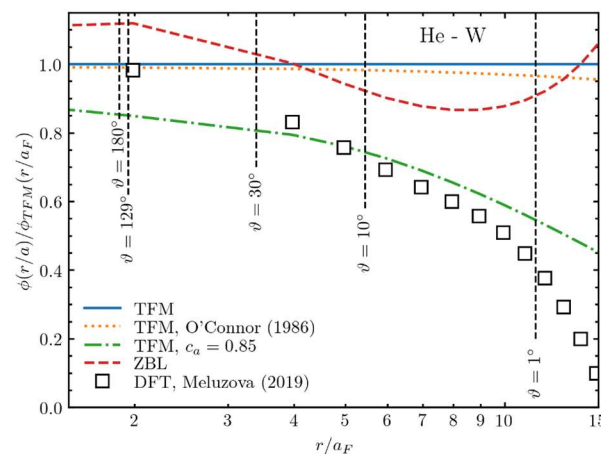


# Interatomic potentials

## Overview of main Results

Ion	$c_a$ (TFM)	
	W(110)	Fe(100)
He	0.85	0.7
D <sub>2</sub>	0.95	≥0.85

- TFM, ZBL and O'Connor deliver better results for cases involving D than He.
- TFM consistently overestimates the interatomic potential.
- O'Connor correction improves the situation but still overestimates the potential.
- ZBL model is better than TFM but still overestimates the potential.
- DFT data agrees well with the experiment for He cases.



P. M. Wolf, E. Pitthan, D. Primetzhofer, submitted for publication (Pinboard 38569)

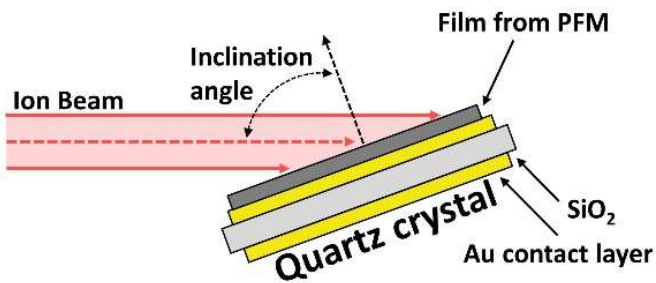




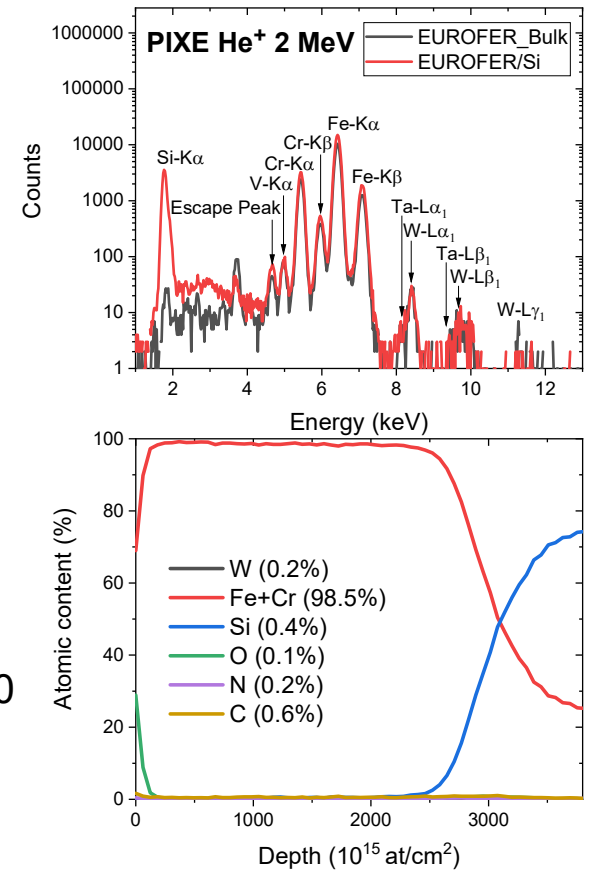
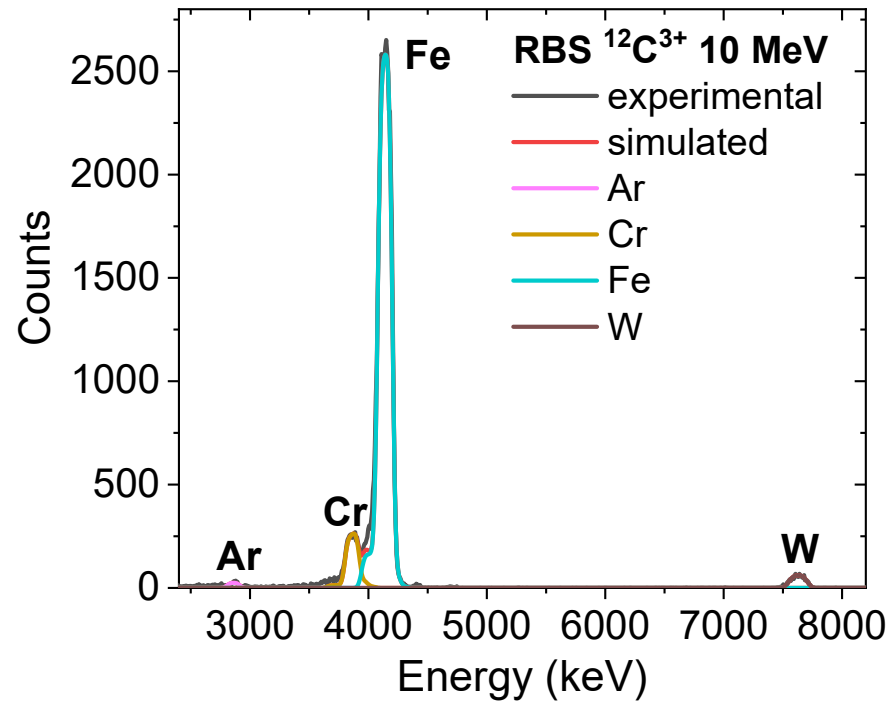
# Sputtering Yields

Experimental approach using high-sensitivity quartz crystal microbalance QCM

## Experimental configuration



Formation and characterization of thin films from EUROFER97 target [1]:



From SIMNRA: Similar composition to bulk.

	At. content (%)	
	Sputtering	Bulk (nominal)
Fe	88.7	88.9
Cr	11.0	9.5
W	0.3	0.3

[1] E. Pitthan, P. Petersson et al. Nucl. Mater. Energy 34 (2023) 101375.



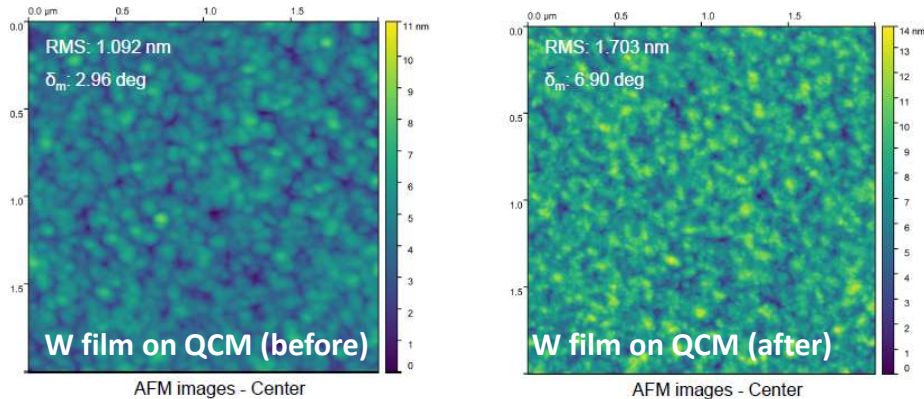


# Sputtering Yields

## Results

→ **AFM measurements before/after measurements:**

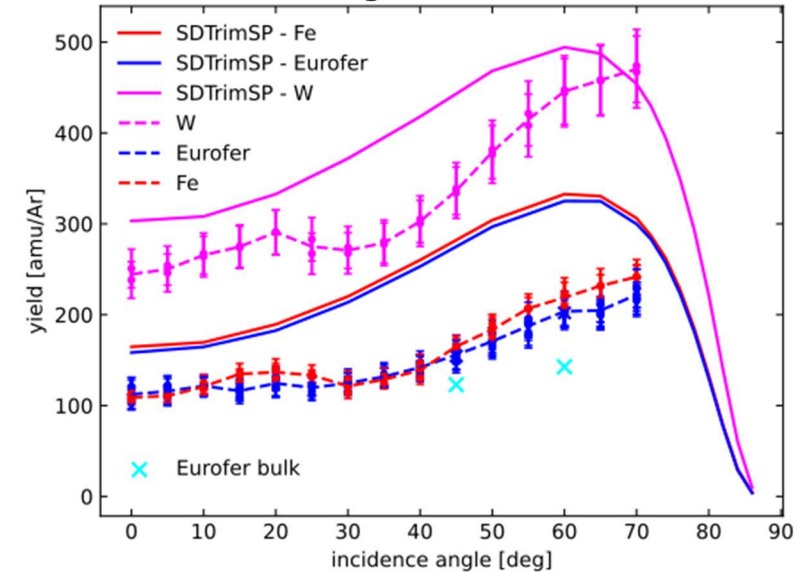
- Typical RMS < 1.8 nm for films;
- homogeneous film growth;
- no significant roughening/smoothing of surface morphology observed after measurements.



→ **Sputtering yield measurements  $\text{Ar}^+$ ,  $\text{D}_2^+$ ,  $\text{He}^+$  bombardment of PFC thin films in different incident angles.**

→ **Bulk (catcher mode) and self-irradiated layers also measured.**

## Irradiation using 2 keV $\text{Ar}^+$ ions



- Poor agreement with default SDTrimSP in all investigated cases (Ar/D on W, Fe and Eurofer).
- Investigate effect of different parameter adjustments in BCA code simulations.

## Additional observations:

- No significant change in self-irradiated samples.
- Smaller SY from EUROFER bulk attributed to roughness.



# Sputtering Yields

Effect of nuclear data corrections in sputtering yield simulations.

## Systematic investigation of effect of nuclear data corrections in sputtering yield simulations.

SDTrimSP (BCA-based) with Graphical User Interface [1]: 1 keV D on Eurofer, Lindhard-Scharff stopping model, Moliere interaction angle potential.

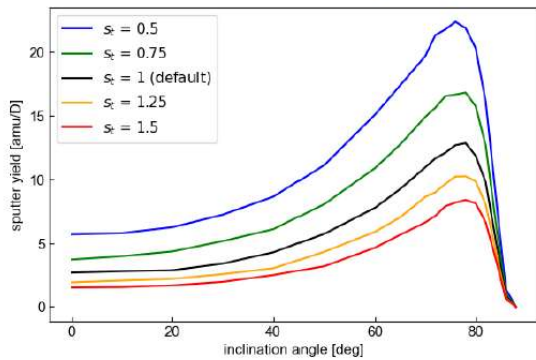
Scaling electronic stopping power;  
Surface binding energy;  
Adsorbate layer thickness;  
Screening length in interatomic potential.

→ global offset in sputtering yields

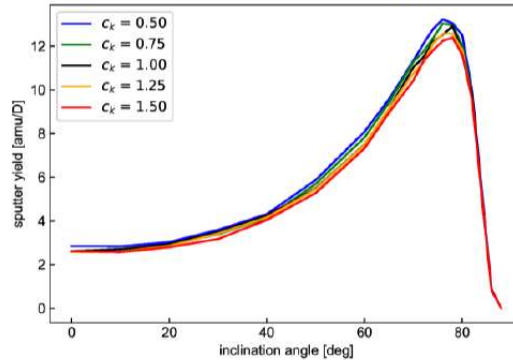
→ offset in sputtering yields

→ Shifted maximum in yields over angle curve

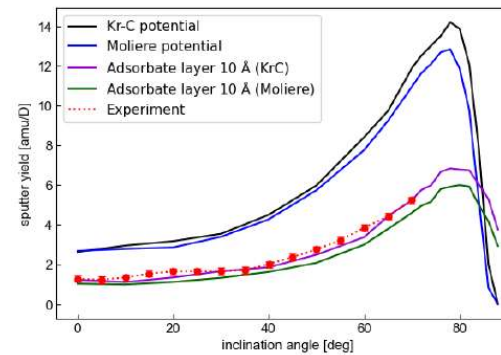
scaled surface binding energy



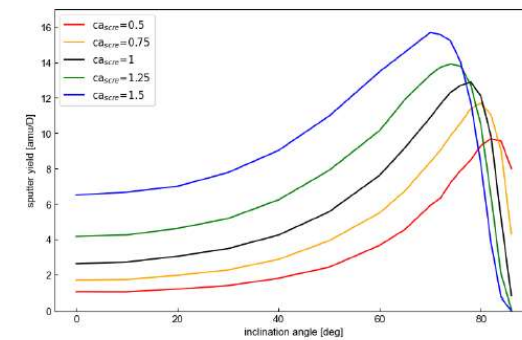
scaled electronic stopping power



adding adsorbate layers



scaled screening length



[1] P. S. Szabo et al. Nucl. Instrum. Methods Phys. Res. B 522 (2022) 47-53.



# Sputtering Yields

Effect of nuclear data corrections in sputtering yield simulations.

Applying energy loss and screening length experimental corrections obtained experimentally in BCA simulations and comparison with experimental sputtering yields.

He 3 keV → W/QCM

## Electronic energy loss model:

Lindhard-Scharff (equivalent to SRIM-13)

Empirical correction  $\times 1.13$

J. Shams-Latifi, et al., Nucl. Mater. and Energy 36 (2023).

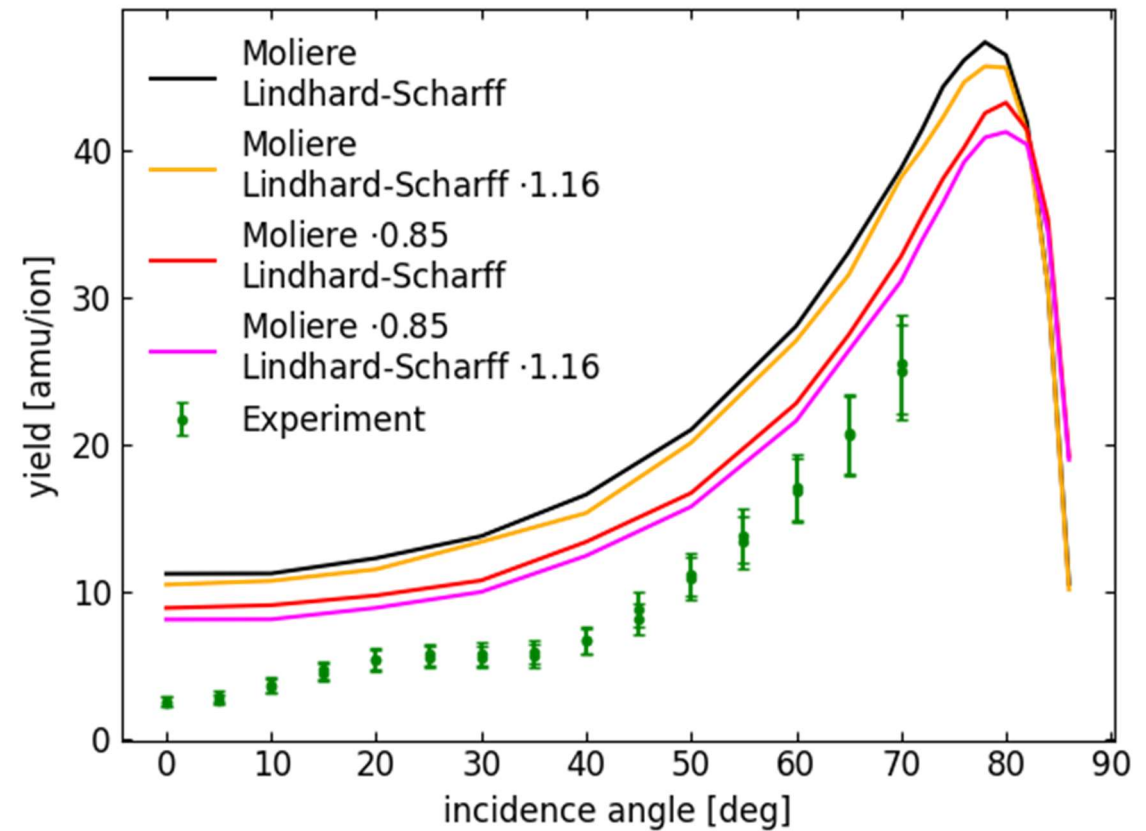
## Interatomic potential model:

Thomas-Fermi-Moliere potential (TFM)

Screening length correction  $\times 0.85$

P. M. Wolf, E. Pitthan, D. Primetzhofer, submitted for publication (Pinboard 38569)

Both corrections lead to a reduction of the sputter yield, going into the direction of the experimental values.





# Sputtering Yields

Effect of surface orientation on sputtering yields

## Experimental observations (TU Wien):

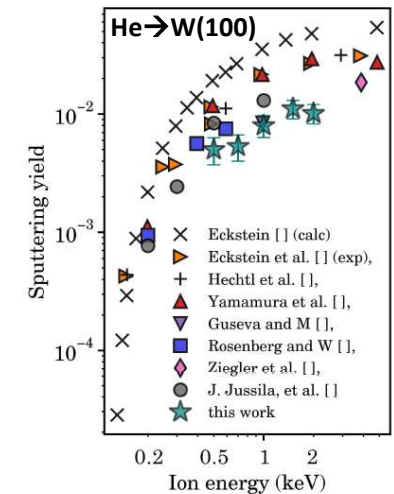
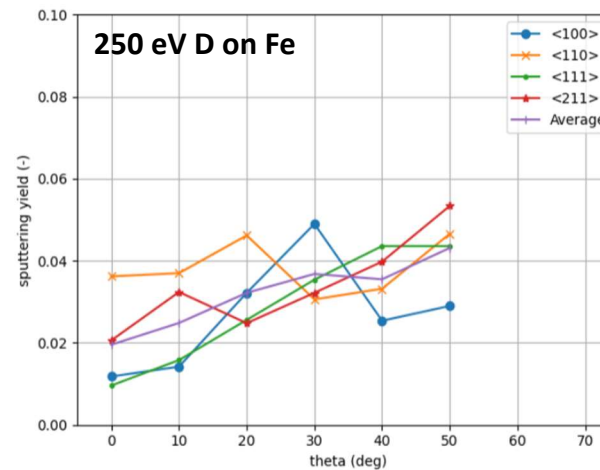
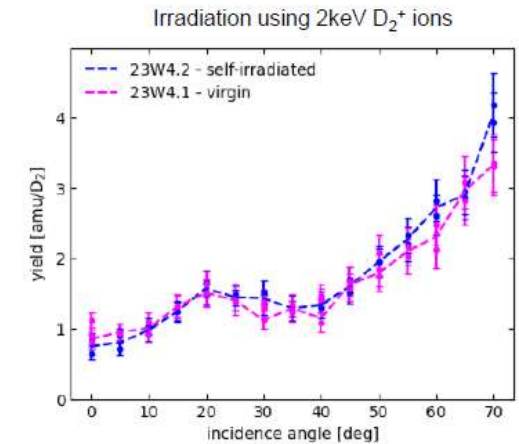
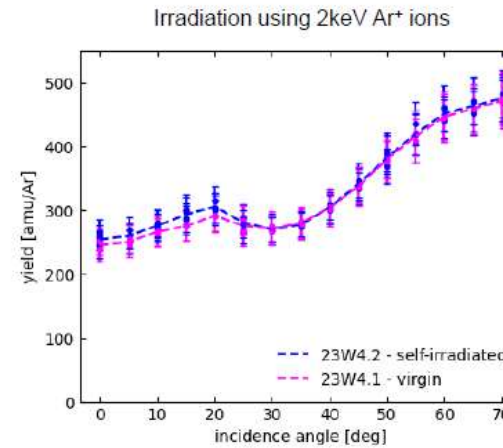
- local minimum in yield over angle curve at around 35 deg incidence angle observed for different measurements for W and Fe layers.
- Possibility of texture and crystallinity effects from preferential grain orientation.
- Detailed theoretical investigation of crystal orientation effect.

## Sputtering with MD simulations (Aalto):

- Effect of surface orientation.
- Effect of surface roughness (step defect).
- Fitting of ion-electron coupling for two temperature model simulations with environmentally dependent stopping power.

## Main observations:

- Dependence on surface orientation (publication under preparation with TUWien).
- Negligible effect of unevenness of surface (step-defect).
- Electronic stopping removes the energy available for sputtering process; all MD-EPH simulations reveal lower yields (under preparation for publication).



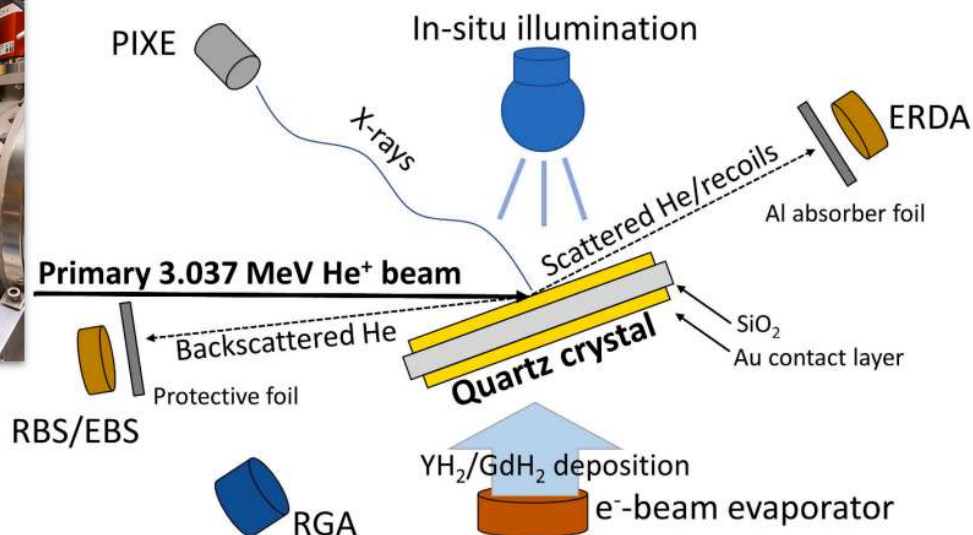
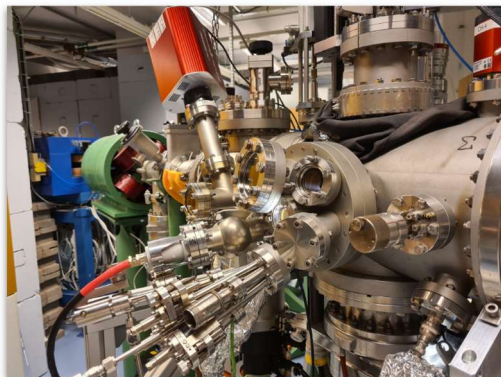




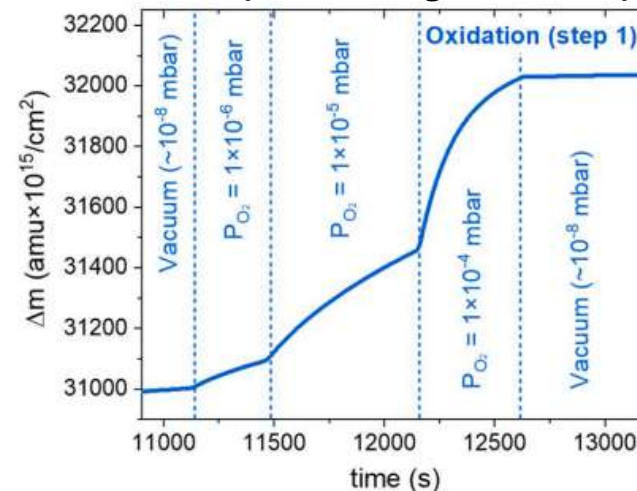
# Sputtering Yields

Implementation of new experimental set-up for in-situ studies

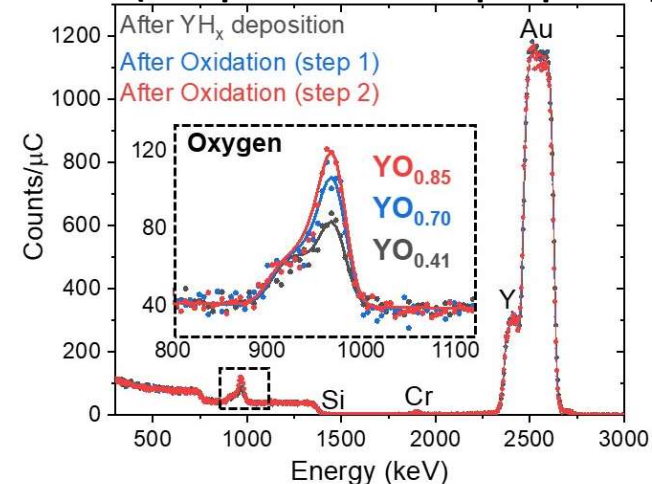
In-situ and real-time mass-change measurements (QCM) and subsequent IBA (RBS, PIXE, ERDA).



QCM (mass changes monitor)



IBA (Composition and depth profile)



Allows in-situ implantation/erosion/deposition/oxidation investigations simultaneous to material characterization by IBA.

Benchmarking: investigation of formation and oxidation of oxygen-containing rare-earth hydrides

E. Pitthan et al. Materialia 27 (2023) 101675.



# Overview

*Main scientific achievements*

## Energy losses

- First experimental data for energy losses of light ions (H, D, and He) in PFC (W, Fe & EUROFER97) at low energies:
- Pronounced discrepancies between semi-empirical models (SRIM-2013) were identified: up to 60% for He in W.
- Detailed TD-DFT calculations (crystal orientation and core-states description) of electronic energy losses for W, Fe, and Fe-Cr: strong crystalline influence and good agreement with previous experimental observations for random geometries.
- No significant effect of defects in experiments and simulations.

## Interatomic potentials

- First experimental measurements of screening length correction for W and Fe and compared to available models:
- Allow assess the quality of models for the interatomic potentials (overall good agreement with recent DFT models).

## Sputtering yields

- New experimental sputtering yields angular dependence for PFC (W, Fe, and re-deposited EUROFER97).
- Detailed investigation of effect of fundamental nuclear data uncertainties in sputtering yield simulations.
- Molecular Dynamic (MD) simulations dependence of crystalline orientation, defects, and electronic effects in SY.
- Integration of real-time mass-change measurements (QCM) in in-situ IBA system.



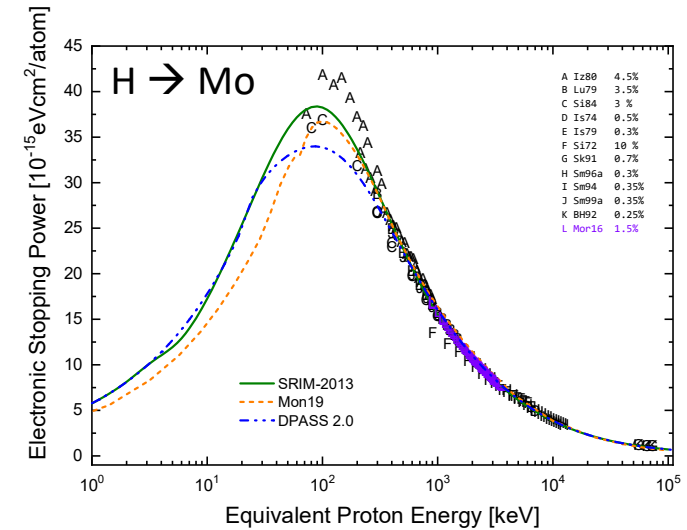
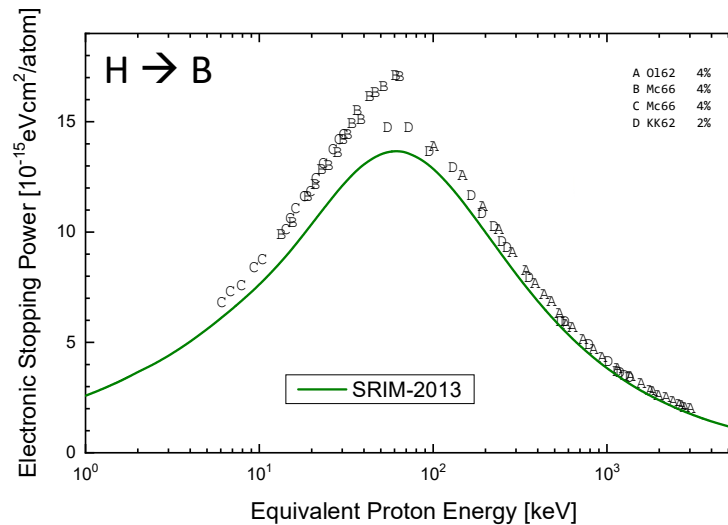
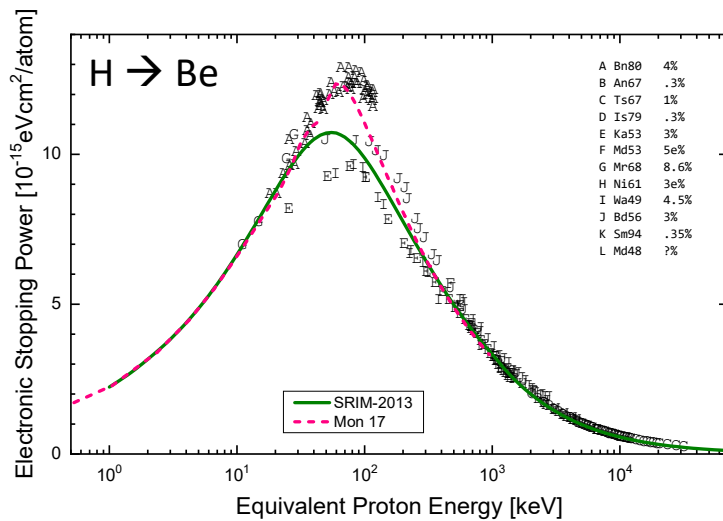


# Overview

## Recommendations:

- To use updated data-sets for fundamental quantities (data is already available in IAEA-most cases).
- Awareness of uncertainties in different combination of ion-matter and potential impact in sputtering yields.

## Other examples related to fusion materials



***Be, B, and Mo: Limited data at low energies and high discrepancy at higher energies.***

***Formation of oxides can lead to larger discrepancies from brags rule: specific studies for compounds are needed.***

***More work is needed on the determination and evaluation of nuclear data for elements and isotopes with relevance for fusion.***



Thank you!



This work has been carried out within the framework of the EUROfusion Consortium, funded by the European Union via the Euratom Research and Training Programme (Grant Agreement No 101052200 — EUROfusion). Views and opinions expressed are however those of the author(s) only and do not necessarily reflect those of the European Union or the European Commission. Neither the European Union nor the European Commission can be held responsible for them.





# Extras





# Ion-irradiation experiments

**Experimental (preparation for WP-3 and 5)**

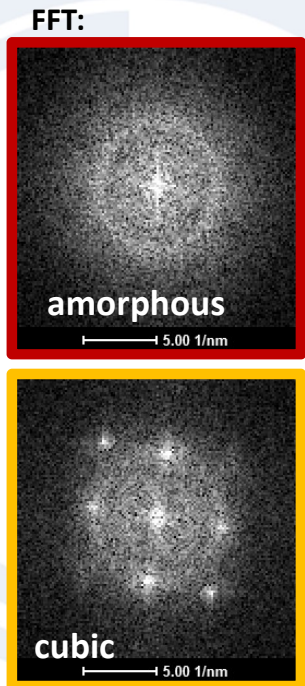
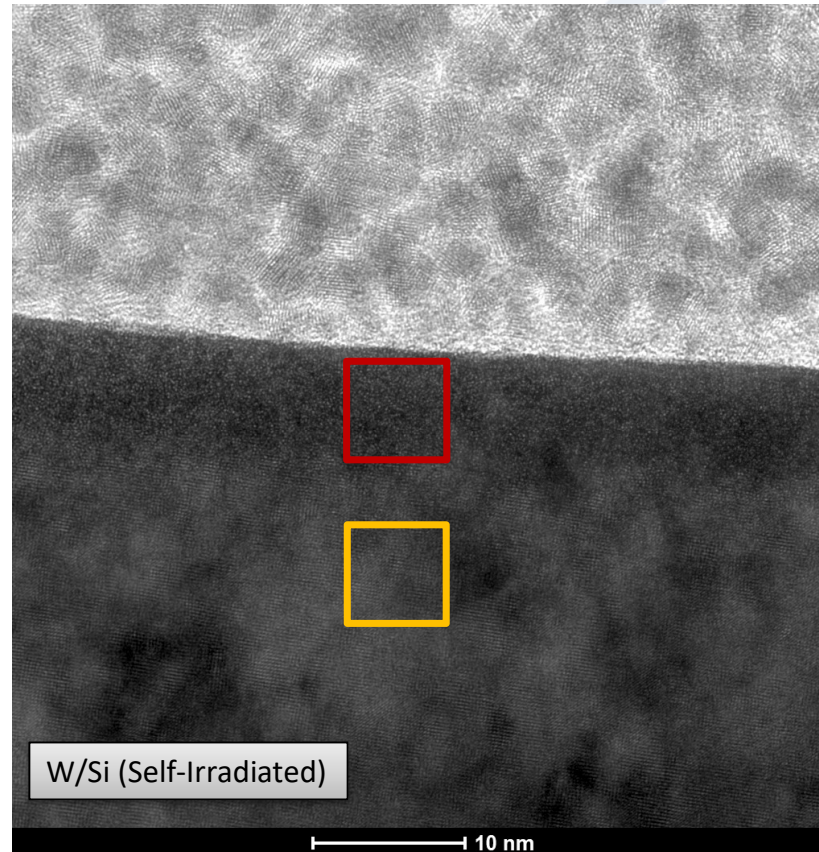
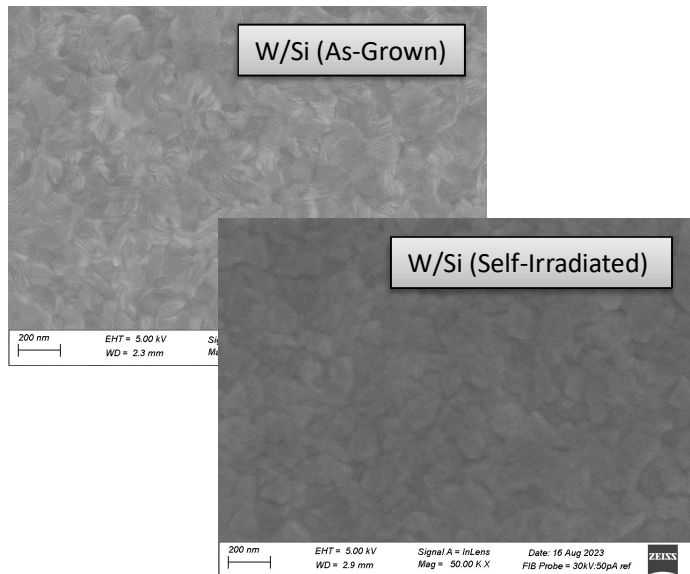
**Sample:** W(300 nm)/(Si, C, QCM)

**Implantation:** W<sup>2+</sup> 600 keV

**Fluence:**  $1.5 \times 10^{15}$  atoms/cm<sup>2</sup>

**SEM:** Smoothing of surface after Implantation.

**TEM:** amorphization of surface.





# Electronic energy loss measurements

Experimental procedure for low energy regime

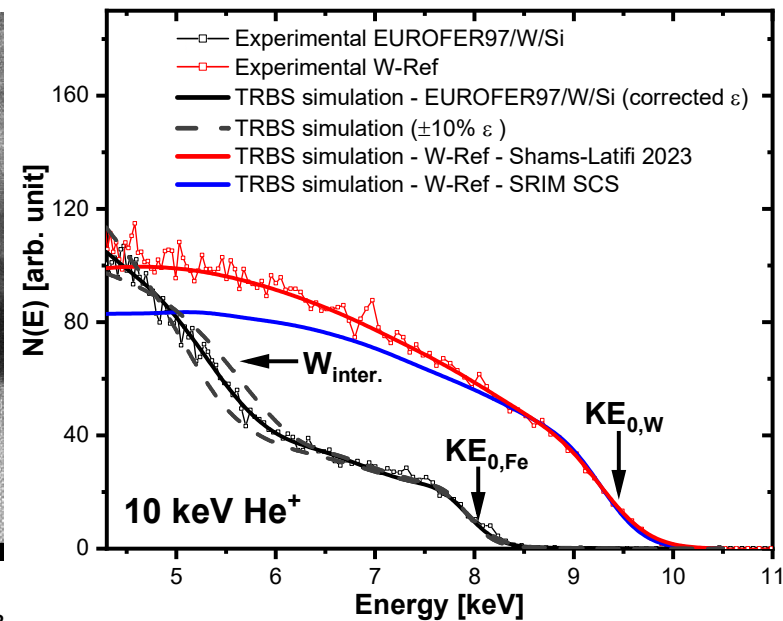
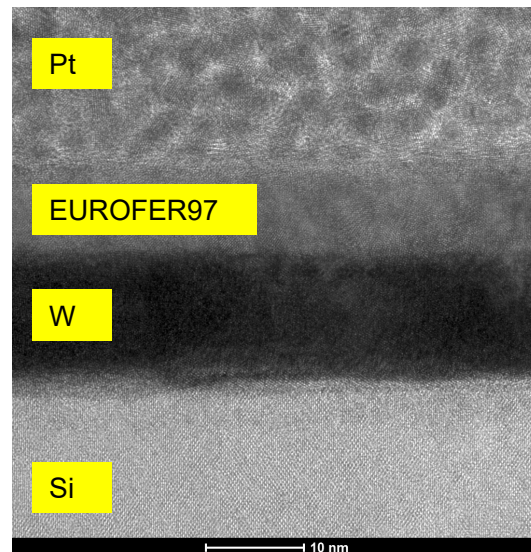
## Complementary approach (marker layer):

Experimental stopping cross-section of sputter-deposited EUROFER97 for LEIS

→ Analysis from spectrum height or spectrum width unfavorable for compound systems and lighter species.

→ Surface interface segregation is a risk – best to look on the signal indirectly – via a marker layer.

### Marker layer:



Characterization of re-deposited PFM structures (pinboard 36144):  
J. Shams-Latifi, E. Pitthan, et. al Mater. Res Express. 11 (2024) 016518.